CRYSTAL GROWTH & DESIGN

ARTICLE

pubs.acs.org/crystal

Structure and Formation of Synthetic Hemozoin: Insights From First-Principles Calculations

Noa Marom,*[,†,‡] Alexandre Tkatchenko,[§] Sergey Kapishnikov,[†] Leeor Kronik,*[,†] and Leslie Leiserowitz*[,†]

[†]Department of Materials and Interfaces, Weizmann Institute of Science, Rehovoth 76100, Israe1

[‡]Center for Computational Materials, Institute for Computational Engineering and Sciences, University of Texas at Austin, Austin, Texas 78712, United States

[§]Fritz-Haber-Institut der Max-Planck-Gesellschaft, Faradayweg 4-6, 14195 Berlin, Germany

ABSTRACT: Malaria, an infectious disease once considered eradicated, has reemerged in recent years, primarily due to parasite resistance to commonly used synthetic antimalarial drugs. These drugs act by inhibiting crystallization of the malaria pigment, hemozoin (HZ). Thus, there is a vital need for understanding the process of HZ nucleation. In a companion paper, the pseudopolymorphic behavior of β-hematin, the synthetic form of HZ, has been characterized by X-ray diffraction (XRD) (Straasø, T.; Kapishnikov, S.; Kato, K.; Takata, M.; Als-Nielsen, J.; Leiserowitz, L. Cryst. Growth Des. 2011, 11, DOI: 10.1021/cg200410b). Here, we employ van der Waals (vdW)-corrected density functional theory (DFT) to study the two β-hematin crystal structures and their repeat unit, a heme dimer. We find that vdW interactions play a major role in the binding of the heme dimer and the β-hematin crystal. In addition, accounting for the periodic nature of the system is essential to obtaining the correct geometry of the heme dimer, which is affected by vdW interactions with adjacent dimers in the β-hematin crystal. The different stereoisomers of the heme dimer and their molecular crystals are close in energy, which is consistent with pseudopolymorphism in β-hematin, in agreement with recent XRD experiments. Finally, we use our results to comment on β-hematin crystallization mechanisms. This work demonstrates the viability of vdW-corrected DFT as a tool for gaining valuable insight into pertinent problems involving biological systems.

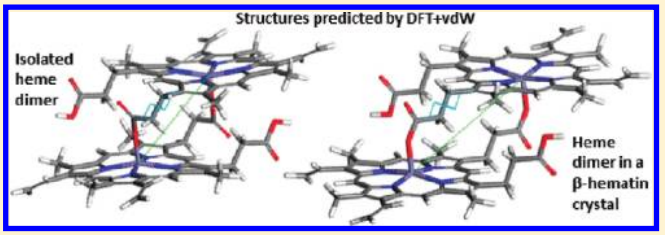

INTRODUCTION

Malaria, an infectious disease once considered eradicated, has reemerged and is regaining strength due to increasing parasite resistance to commonly used synthetic antimalarial drugs.[1] Hence, there is an ever-growing need for developing new and more efficient drugs. During the course of malaria, the parasite enters the red blood cell, where it feeds on hemoglobin, releasing the heme as a byproduct. The parasite avoids the toxicity of heme by promoting its crystallization into nonreactive hemozoin (HZ). This takes place in a designated organelle, known as the digestive vacuole. Quinoline-based antimalarial drugs work by inhibiting the nucleation/growth of HZ crystals.[2−7] Therefore, understanding the mechanisms of HZ crystallization and its inhibition is an effective strategy in the battle against malaria.

Many open questions remain regarding the mechanisms of HZ nucleation and growth.[3,8−15] The room temperature crystal structure of the synthetic form of HZ, β-hematin, has been determined via X-ray powder diffraction (XRD).[6] β-Hematin, depicted in Figure 1, has a triclinic unit cell. The repeat unit is a centrosymmetric heme [ferriprotoporphyrin IX (Fe(3+) PPIX)] cyclic dimer (*cd*), where the two molecules are linked through iron−carboxylate bonds between the propionate side chain of one molecule and the central Fe atom of the other. The free propionic acid groups of the cyclic dimers form hydrogen bonds along the $[10\bar{1}]$ direction. Along the [010] direction, the dimers are π-stacked in a similar formation to that typical of molecular crystals of porphyrins and phthalocyanines,[16] albeit with a larger interplanar distance and a smaller lateral overlap between the porphyrin moieties. Additional stabilization is gained from the dispersion interactions between the methyl and the vinyl side chains of adjacent dimers.

Pagola et al.[6] have reported that β-hematin is composed only of the centrosymmetric dimer, denoted here as $cd\bar{1}_1$, where $\bar{1}$ symbolizes the inversion symmetry element. However, from symmetry considerations, one may envisage the formation of additional stereoisomers of the heme dimer: a second centrosymmetric dimer, denoted as $cd\bar{1}_2$, a chiral noncentrosymmetric dimer, denoted as *cd*2 (where 2 symbolizes the pseudo-2-fold symmetry relating the two monomers), and its enantiomer.[17] The stereoisomers are depicted in Figure 2, and the differences are apparent in the positions of the methyl and vinyl side groups on the two heme monomers. This gives rise to the question of the possible presence of stereoisomers other than the observed $cd\bar{1}_1$. A clue to the presence of a second phase of β-hematin has been observed by Bohle et al., based on powder diffraction data,[14] but only now, Straasø et al.[18] have succeeded in identifying and determining the structure of a minor phase of β-hematin, which

Received: April 1, 2011
Published: June 02, 2011

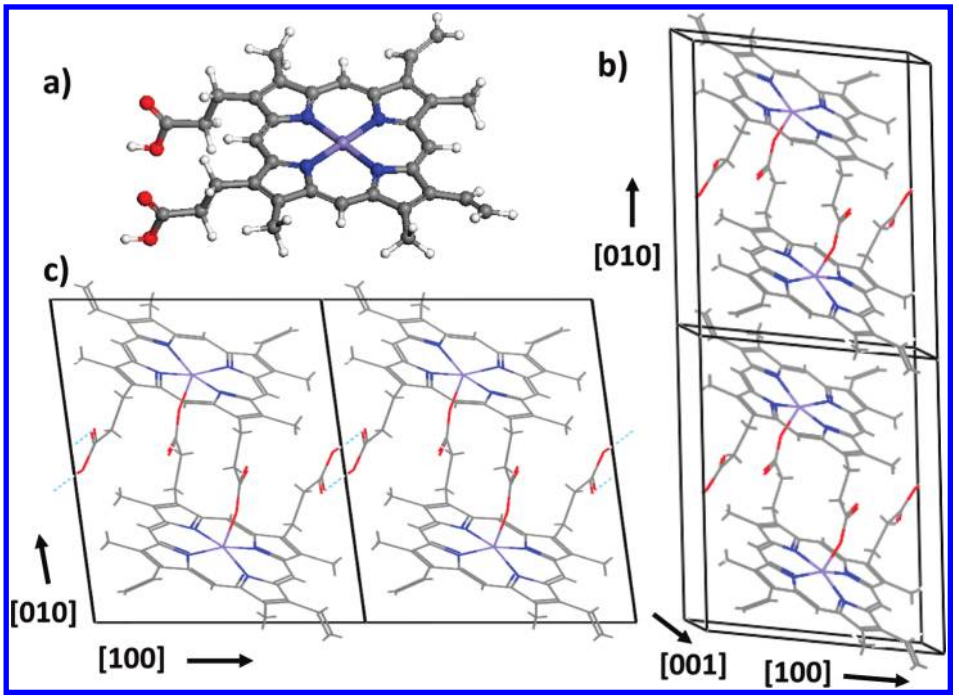

Figure 1. Schematic illustration of the structure of the β-hematin molecular crystal (only the unit cell of the major phase is shown): (a) the Fe(3+) PPIX (heme) monomer, (b) stacking of the Fe(3+) PPIX dimers along the [010] direction, and (c) the hydrogen bond between the free propionic acid groups along the $[10\bar{1}]$ direction. C atoms are shown in gray, N in blue, O in red, Fe in violet, and H in white. In some of the illustrations, hydrogen atoms are not shown for clarity.

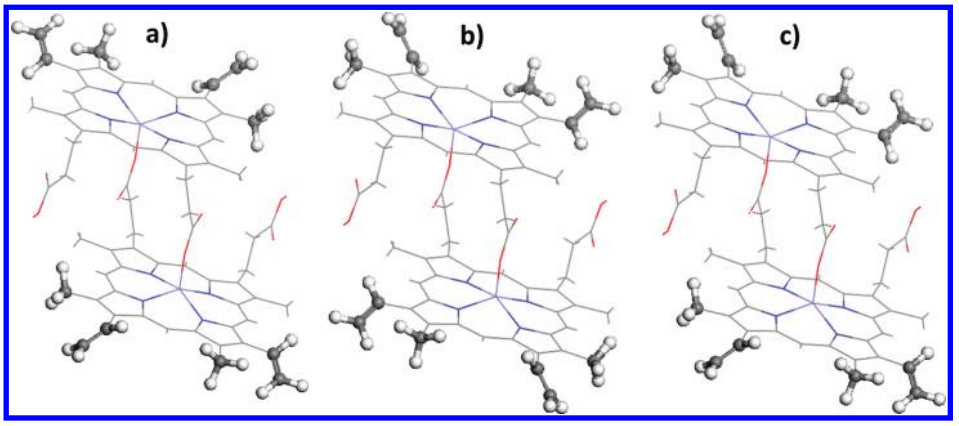

Figure 2. Schematic illustration of the different steroisomers of the Fe(3+) PPIX dimer: (a) centrosymmetric $cd\bar{1}_1$, (b) centrosymmetric $cd\bar{1}_2$, and (c) noncentrosymmetric chiral $cd2$. The differences are apparent in the positions of the methyl and vinyl side groups on the two Fe(3+) PPIX monomers.

is associated with the $cd\bar{1}_2$ stereoisomer. Recently, Klonis et al.[19] have conducted an XRD study of biogenic HZ and proposed a mechanism whereby the nucleation begins with the formation of $\pi-\pi$ Fe(3+) PPIX dimers, rather than cyclic dimers. However, they do not address the possibility of formation of different stereoisomers of the cyclic dimer and the subsequent formation of two distinct crystalline phases.

The analysis of powder XRD data from molecular crystals is a challenging task, and the results are given to interpretation as some assumptions must be made regarding the internal parameters to determine the unit cell structure. In the Pagola et al.[6] refinement of β-hematin, the structure of the heme monomer unit was based on that of chlorohemin[20] and kept rigid. Clearly, such assumptions affect the final outcome of the analysis (see further discussion in ref 18). Therefore, first-principles computational modeling of the different stereoisomers and their crystal structures allows us to gain insight beyond what is possible by experimental means only. Density functional theory (DFT)[21] is clearly the first-principles method of choice for systems of this size, as it offers good accuracy at an affordable computational cost.

There is an extensive body of literature, too vast to review here in detail, on DFT calculations of the electronic structure of iron porphyrins and phthalocyanines, which are chemically similar to Fe(3+) PPIX. Iron porphyrins are often used to emulate the interaction of heme with various species,[22−45] while works on Fe(3+) PPIX remain relatively scarce.[46−49] Notably, Charkin et al.[50] have calculated the structure of a centrosymmetric Fe(3+) PPIX dimer and its ion. However, they used an exchange-correlation

Table 1. Relative Energies with Respect to the $cd\bar{1}_1$ Stereoisomer in the J = 11 Spin State, vdW Correction, and Binding Energies with Respect to Two Fe(3+) PPIX Monomers and a Hydrogen Molecule for the Three Stereoisomers of the Fe(3+) PPIX Dimer, Fully Relaxed Using PBE+vdW

		$cd\bar{1}_1$		$cd\bar{1}_2$		$cd2$	
J		7	11	7	11	5	11
				PBEh+vdW			
relative energy	eV	0.28	0.00	0.53	0.14	0.49	0.03
	kcal/mol	6.42	0.00	12.29	3.26	11.29	0.59
vdW correction	eV	−4.20	−4.11	−4.07	−4.00	−4.05	−3.92
	kcal/mol	−96.82	−94.66	−93.84	−92.33	−93.35	−90.31
BE w/r to 2*heme−H_2	eV	−1.18	−1.46	−0.93	−1.32	−0.97	−1.43
	kcal/mol	−27.25	−33.67	−21.38	−30.41	−22.38	−33.08
				PBE+vdW			
relative energy	eV	−0.86	0.00	−0.70	0.10	−0.50	0.05
	kcal/mol	−20.41	0.00	−16.22	2.35	−11.43	1.08
vdW correction	eV	−4.54	−4.45	−4.42	−4.36	−4.39	−4.25
	kcal/mol	−104.79	−102.57	−101.95	−100.45	−101.24	−98.05
BE w/r to 2*heme− H_2	eV	−1.07	−0.19	−0.89	−0.09	−0.68	−0.14
	kcal/mol	−24.76	−4.34	−20.57	−1.99	−15.77	−3.27

functional based on semilocal correlation. Such functionals inherently lack treatment of dispersion interactions, which are a long-range correlation effect. In addition, the dimer structures that they suggest involve a *syn*-planar O = C−O−Fe(3+) conformation as opposed to the observed *anti*-planar configuration. To the best of our knowledge, computational studies of the different stereoisomers of the Fe(3+) PPIX cyclic dimer and of crystalline β-hematin have not yet been conducted.

Recently, significant progress has been made toward including dispersion interactions in DFT (see, for example, refs 51 and 52). Here, we present a dispersion-corrected DFT study of β-hematin, using the Tkatchenko−Scheffler vdW (TS-vdW) correction.[53] Within this approach, the long-range leading order of the dispersion energy, C_6/R^6, is added in a pairwise manner to the internuclear energy term. The C_6 coefficients and the vdW radii are determined in a parameter-free fashion from the DFT ground state electron density and reference values for the free atoms. The only empirical parameter in the TS-vdW scheme is the range of the damping function used to avoid unnecessary short-range dispersion corrections, which is determined once per functional by fitting to the S22 data set of weakly interacting complexes. Advantageously, this scheme can be coupled to the functional most suitable for describing the electronic structure and chemical bonding.[54] The TS-vdW scheme has been used successfully to describe the electronic structure and dispersion interactions in metal-phthalocyanine dimers, which are chemically related to heme.[54] In addition, it has been applied to a data set of noncovalently interacting dimers,[53] water clusters,[55] biomolecules,[56] organic/inorganic interfaces,[57,58] graphene nanoribbons,[59] and layered inorganic compounds.[60] In most of these cases, the TS-vdW scheme coupled with an appropriate DFT functional has yielded results on par with highly accurate but computationally much more expensive, quantum-chemical and many-body methods that rely on explicit treatment of long-range correlation. The efficiency of the TS-vdW scheme makes the electronic structure calculations and geometry relaxations of large systems feasible, including a fully periodic treatment of the β-hematin crystal.

In this article, we show that correctly accounting for dispersion interactions is essential to obtaining the correct geometry of both the β-hematin crystal and its repeat unit, the Fe(3+) PPIX cyclic dimer. In addition, the structure of the cyclic dimer in β-hematin is affected by the crystalline environment through dispersion interactions with adjacent dimers. Our findings, regarding the relative stability of the three stereoisomers of the cyclic Fe(3+) PPIX dimer as isolated dimers and in the unit cells of the two phases of β-hematin, lead us to suggest a mechanism in which the nucleating unit is a cyclic dimer. The formation of more than one stereoisomer in the dimerization stage followed by segregation in the growth stage explains the formation of two distinct phases of β-hematin, associated with different stereoisomers of the cyclic heme dimer.

MATERIALS AND METHODS

DFT calculations were performed using the generalized gradient approximation (GGA) of Perdew, Burke, and Ernzerhof (PBE)[61] and with the one-parameter PBE-based hybrid functional (PBEh), with 25% of Hartree−Fock exchange.[62,63] To account for dispersive interactions, both functionals were augmented with the TS-vdW correction.[53,54] All calculations were performed with the FHI-aims code,[64,65] using the tier2 numerical atomic-centered orbital (NAO) basis set,[66] which has been demonstrated to approach the basis set limit and be nearly free of basis set superposition errors (BSSE).[64] It has also yielded results similar in accuracy to those of the aug-cc-pVQZ Gaussian basis set for a data set of noncovalently interacting dimers.[53] The constrained-DFT formalism of Behler et al.[67,68] was used for conducting spin-restricted calculations.

RESULTS AND DISCUSSION

Cyclic Fe(3+) PPIX Dimer. If the crystallization of β-hematin begins with Fe(3+) PPIX dimerization, then the relative stability of the isolated dimers will determine which stereoisomers form and in what quantity. Therefore, we first examine the three stereoisomers as isolated dimers and then proceed to examine

Table 2. Structural Parameters of the Three Stereoisomers of the Isolated Fe(3+) PPIX Dimer Obtained from Full Relaxation with PBE+vdW as Compared to the Structures Obtained from Refinement of X-ray Diffraction Data[a]

	$cd\bar{1}_1$		$cd\bar{1}_2$		$cd2$			Straasø et al.[18]	
J	7	11	7	11	5	11	Pagola et al.[6]	major	minor
interplanar distance (Å)	4.82	4.91	5.17	5.03	∼4.46	∼4.92	4.60	4.59	4.57
mean deviation from planarity (Å)	0.12	0.11	0.12	0.08	0.15	0.04	0.11	0.03	0.03
					0.08	0.03			
Fe shift from porphyrin plane (Å)	0.27	0.48	0.23	0.44	0.21	0.47	0.55	0.49	0.46
					0.26	0.49			
Fe−Fe distance (Å)	7.03	6.81	8.63	8.53	8.49	8.39	9.05	8.94	9.24
Fe−O bond length (Å)	1.94	1.89	1.92	1.87	1.85	1.88	1.89	1.84	1.85
					1.92				
O−C−O−Fe torsion angle	133.97	129.5	100.3	112.7	136.1	116.8	155.2	167.5	155.7
					82.7	128.5			
C−C−C−C torsion angle on propionate bridge	86.6	85.9	176.6	175.1	92.8	111.8	171.2	174.6	172.8
					116.9	112.0			
C−C−C−C torsion angle on propionic acid	176.9	177.2	175.6	173.9	170.1	166.5	157.3	166.7	162.8
					174.8	175.1			

[a] The interplanar distance, the mean deviation from planarity, and the Fe shift are given with respect to the planes of the porphyrin skeletons without the Fe atom and the side groups, obtained by principal component analysis. Two values are shown if the relaxed structure is not completely symmetric, as a center of symmetry was not imposed. If the planes of the two monomers are not perfectly parallel, the interplanar distance is approximate.

them in crystalline form. The structures of the two centrosymmetric stereoisomers of the Fe(3+) PPIX cyclic dimer (depicted in Figure 2) were relaxed using PBE+vdW, with and without constraining the spin to the experimentally observed high spin state with $J = 11$.[69,70] The initial geometry was taken from the refined low-temperature (90° K) structure obtained by Straasø et al.,[18] with the COOH carboxyl group on the free propionic acid oriented such that the −C═C−C═O moiety adopts the more commonly observed *syn*-planar conformation, rather than being *anti*-planar, as assumed by Pagola et al.[6] Table 1 shows the relative energy, the vdW contribution, and the binding energy with respect to various species of the three stereoisomers. The relative energies are given with respect to $cd\bar{1}_1$ in the $J = 11$ state. There is a well-known difficulty in treating the multiplet structure of intermediate and high-spin systems with commonly used exchange correlation functionals. This has been demonstrated for various iron-containing complexes,[71] for iron phthalocyanine,[72] and for Fe(3+) PPIX and similar iron porphyrins.[24−26,28,30,31,33,36,42−46] Specifically, (semi)local functionals, such as PBE, tend to favor lower spin configurations than hybrid functionals such as PBEh. This tendency is seen here for the heme dimer, where PBEh+vdW gives the correct high-spin configuration with $J = 11$, while PBE+vdW favors the $J = 7$ configuration for the two centrosymmetric stereoisomers and the $J = 5$ configuration for the noncentrosymmetric stereoisomer. Adding the vdW correction does not affect the behavior of the parent functional in this respect. Fortunately, for all cases studied here, the spin state has only a minor effect on the geometry of the system (further elaborated below), and the relative stability of the different stereoisomers is obtained from spin unconstrained calculations. Therefore, we are able to draw valid conclusions from DFT calculations despite the inaccuracies in predicting the spin state.

Both PBE+vdW and PBEh+vdW predict that the $cd\bar{1}_1$ stereoisomer is indeed the most stable (for the respective lowest energy spin configuration obtained with each functional). However, PBE+vdW predicts that the $cd\bar{1}_2$ isomer is the second most stable, in agreement with the findings of Straasø et al.,[18] while PBEh+vdW predicts that the $cd2$ isomer is the second most stable. In this regard, we note that the PBEh+vdW calculations are single point calculations conducted for the geometry obtained using PBE+vdW, and further geometry relaxation may affect the relative energies of the stereoisomers. The energy differences between the stereoisomers, on the order of 0.1 eV (2 kcal/mol), are generally quite small and are consistent with the possible formation of all three stereoisomers. In addition, the relative stability of the different stereoisomers may be affected by the nucleation environment, for example, through solvent effects, which are not taken into account here.

The vdW correction has a significant contribution of 4−4.5 eV (90−105 kcal/mol) to the energy of the Fe(3+) PPIX dimers, and it plays an important role in the relative stability of the stereoisomers. In fact, attempting to relax the structure of a dimer using PBE without the vdW correction yielded a distorted geometry, where one monomer is significantly tilted with respect to the other, and all semblance of symmetry is lost. Table 2 shows some structural parameters of the Fe(3+) PPIX dimers relaxed with PBE+vdW, as compared to the structure of the $cd\bar{1}_1$ stereoisomer, the predominant stereoisomer in β-hematin, obtained by Pagola et al.,[6] and to the structure of both stereoisomers, obtained by Straasø et al.[18] Relaxation of the isolated dimers using PBE+vdW generally yielded structures where the porphyrin rings of the two monomers have a greater overlap than that observed in β-hematin. This is reflected in the Fe−Fe distances, which are shorter than those found by Pagola et al. and by Straasø et al., although the interplanar distance between the porphyrin rings is not smaller. For lack of any other interactions with the environment, dispersion interactions pull the π-systems of the two monomers closer together. To bring the two monomers into a greater overlap, the bridging propionate chains are no longer fully extended. This is reflected in the smaller C−C−C−C torsion angle, which is closer to 100° for the $cd\bar{1}_1$ and $cd2$ dimers, rather than close to 180°, as expected for a fully extended chain. For the free propionic acids, the C−C−C−C torsion angle is close to 180°, as they are indeed fully

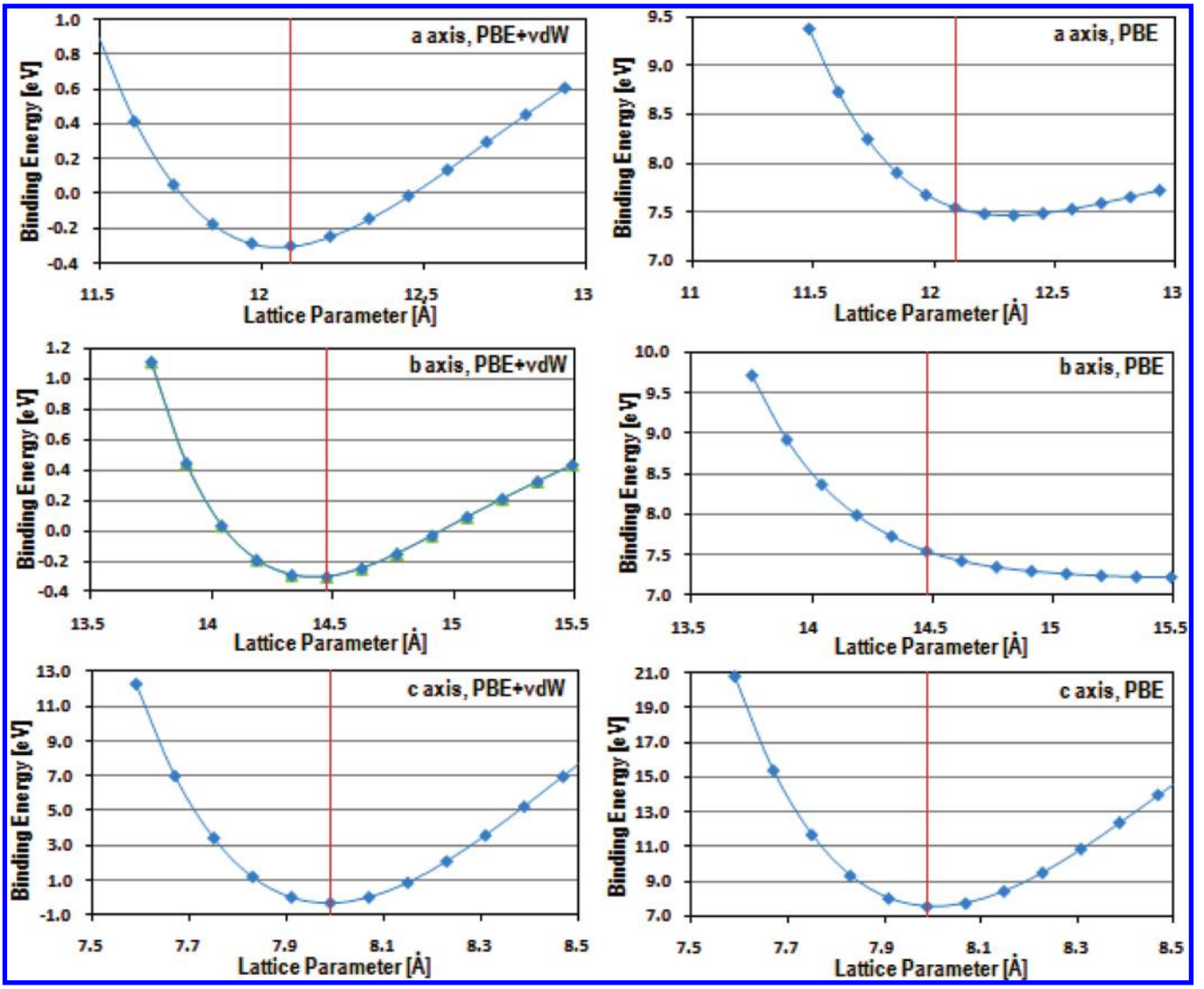

Figure 3. Binding energy with respect to a free Fe(3+) PPIX dimer vs lattice parameter along the three crystal axes of the major phase ($cd\bar{1}_1$) of β-hematin, obtained with PBE+vdW and with uncorrected PBE. The experimental lattice parameters obtained by Straasø et al.[18] are indicated by red lines.

extended. In addition, the O = C−O−Fe(3+) torsion angles are also closer to 100° than to 180°.

***β*-Hematin Molecular Crystal.** Having investigated the isolated dimers, we now proceed to the formation of the molecular crystal. First, we focus on assessing the contribution of weak interactions, that is, dispersion and hydrogen bonds, to the stabilization of the crystal. For this purpose, we use the refined structure of the major phase of β-hematin, $cd\bar{1}_1$, as obtained by Straasø et al.,[18] with the lattice parameters a = 12.089 Å, b = 14.474 Å, c = 7.989 Å, α = 90.82°, β = 96.8°, and γ = 97.64°.[73] The lattice parameters were changed manually, one at a time, around the experimental values to obtain binding energy curves along the different crystal axes. Figure 3 shows the binding energy curves, with respect to free Fe(3+) PPIX, obtained using PBE and PBE+vdW, without relaxing the internal parameters of the heme dimer. The equilibrium lattice parameters obtained with PBE+vdW are very close to the experimental values along all crystal axes. In contrast, uncorrected PBE exhibits a markedly different behavior along the different directions. Along the c-axis, where the binding is predominantly due to hydrogen bonds between the free propionic acids of adjacent dimers, the minimum of the energy curve is considerably deeper than along the other directions. Along this direction, PBE behaves similarly to PBE+vdW and gives an equilibrium lattice parameter in agreement with experiment. Indeed, it is well-known that GGA functionals can provide a reasonable description of all but the weakest hydrogen bonds.[21] However, along the a-axis, PBE gives a shallow minimum and significantly overestimates the lattice constant. This is because along this direction the contribution of the hydrogen bonds is smaller and the binding is mostly due to dispersion interactions between the methyl and the vinyl side groups of adjacent dimers. Worse, along the b-axis, where the binding is predominantly due to dispersive $\pi-\pi$ interactions between the porphyrin rings of adjacent dimers, uncorrected PBE gives no minimum at all. We therefore conclude that accounting for dispersion interactions is essential for describing the structure of β-hematin and similar molecular crystals.

Following the demonstration of the contribution of the vdW correction toward obtaining the correct unit cell structure, the three stereoisomers of the cyclic dimer were placed in the unit

cells of the major and minor phases of β-hematin. The lattice parameters of the low-temperature (90 K) minor phase, as obtained by Straasø et al.,[18] are a = 12.442 Å, b = 15.095 Å, c = 7.638 Å, α = 99.84°, β = 97.11°, and γ = 93.36°.[73] The internal parameters of the geometry were fully relaxed using PBE+vdW both in the experimentally observed high-spin state and in the lower spin state favored by PBE+vdW. Figure 4 shows the superimposed structures obtained for the $cd\bar{1}_1$ stereoisomer in the unit cell of the major phase of β-hematin in both spin states.

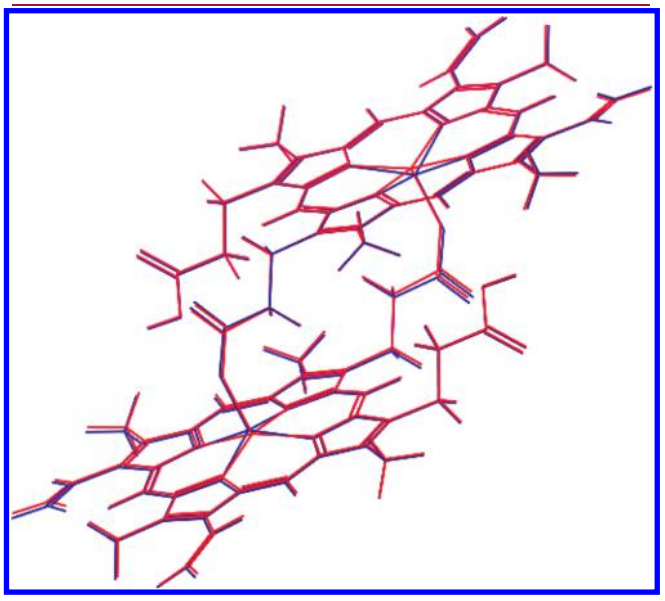

Figure 4. Superimposed relaxed structures of the Fe(3+) PPIX dimer in the unit cell of the major phase of β-hematin, with spin multiplicities of J = 11 in blue and J = 7 in red. The main difference is in the shift of the Fe atom from the porphyrin plane.

The spin multiplicity has only a minor effect on the geometry. Mainly, for the higher spin state, the Fe atoms are shifted farther out of the porphyrin planes and toward each other. This is also apparent for the other isomers and for the isolated dimers.

Table 3 shows the relative energy, the vdW contribution, and the binding energy with respect to free heme and with respect to an isolated dimer in the same spin state, of the three stereoisomers in crystalline form. The relative energies are given with respect to the $cd\bar{1}_1$ stereoisomer in the unit cell of the major phase in the J = 11 state. The ordering of the spin states remains unaffected by the transition from an isolated dimer to a crystal. Generally, the binding energy of the crystal with respect to the dimer is about the same as the difference in the vdW energy component of the two. This is yet another indication for the importance of dispersion interactions to the stabilization of β-hematin. In both unit cells, the $cd\bar{1}_1$ stereoisomer is the most stable, followed by $cd2$ stereoisomer, and the $cd\bar{1}_2$ stereoisomer is the least stable. The spin state does not affect the relative stability of the stereoisomers. Interestingly, the $cd\bar{1}_2$ stereoisomer is more stable in the minor phase unit cell than in the major phase unit cell, while the $cd\bar{1}_1$ and $cd2$ stereoisomers are more stable in the major phase unit cell. This is consistent with the formation of the major phase by the $cd\bar{1}_1$ stereoisomer and the minor phase by the $cd\bar{1}_2$ stereoisomer. A third phase of β-hematin has not been observed to the best of our knowledge.[74] From stereochemical[18] and thermodynamic considerations, the $cd2$ stereoisomer is likely occluded into the major phase.Table 4 shows some structural parameters of the relaxed β-hematin stereoisomers in both unit cells, as compared to the refined structure of the major phase as obtained by Pagola et al.[6] and to the refined structures of the major and minor phases obtained by Straasø et al.[18] Figure 5 shows the relaxed structures of the $cd\bar{1}_1$ stereoisomer as an isolated dimer and in the unit cell of the major phase. The main difference between the structures of the isolated dimers and the

Table 3. Relative Energies with Respect to the $cd\bar{1}_1$ Stereoisomer in the Major Phase Unit Cell in the J = 11 Spin State, vdW Correction, and Binding Energies with Respect to a Relaxed Isolated Dimer in the Same Spin State for the Three Stereoisomers in the Unit Cells of the Major and Minor Phases, Following Relaxation of the Internal Parameters Using PBE+vdW

		$cd\bar{1}_1$		$cd\bar{1}_2$		$cd2$	
J		7	11	7	11	7	11
				in the unit cell of the major phase			
relative energy	eV	−0.85	0.000	−0.12	0.69	−0.54	0.37
	kcal/mol	−19.57	0.000	−2.80	16.00	−12.37	8.62
vdW correction	eV	−10.37	−10.41	−10.34	−10.37	−10.36	−10.38
	kcal/mol	−239.12	−240.04	−238.52	−239.12	−238.91	−239.28
BE/unit cell w/r to 2*heme−H_2	eV	−7.41	−6.57	−6.69	−5.88	−7.11	−6.20
	kcal/mol	−171.10	−151.53	−154.33	−135.53	−163.90	−142.91
BE/unit cell w/r to a dimer with the same J	eV	−6.35	−6.38	−5.80	−5.79	−6.42	−6.06
	kcal/mol	−146.34	−147.19	−133.76	−133.54	−148.13	−139.64
				in the unit cell of the minor phase			
relative energy	eV	−0.41	0.42	−0.23	0.67	−0.29	0.59
	kcal/mol	−9.35	9.68	−5.41	15.53	−6.64	13.74
vdW correction	eV	−10.19	−10.22	−10.18	−10.20	−10.22	−10.246
	kcal/mol	−234.87	−235.77	−234.64	−235.10	−235.75	−236.28
BE/unit cell w/r to 2*heme−H_2	eV	−6.98	−6.15	−6.81	−5.90	−6.86	−5.97
	kcal/mol	−160.88	−141.85	−156.94	−136.00	−158.17	−137.79
BE/unit cell w/r to a dimer with the same J	eV	−5.90	−5.96	−5.91	−5.81	−6.17	−5.83
	kcal/mol	−136.12	−137.50	−136.37	−134.01	−142.39	−134.52

dx.doi.org/10.1021/cg200409d |Cryst. Growth Des. 2011, 11, 3332–3341

Table 4. Structural Parameters of the Three Stereoisomers in the Unit Cells of the Major and Minor Phases, as Obtained from Relaxation of the Internal Parameters with PBE+vdW, as Compared to the Structures Obtained from Refinement of X-ray Diffraction Data[a]

	$cd\bar{1}_1$		$cd\bar{1}_2$		$cd2$			
J	**7**	**11**	**7**	**11**	**7**	**11**	Pagola et al.[6]	Straasø et al.[18]
				in the unit cell of the major phase				
interplanar distance (Å)	4.62	4.66	~4.46	~4.54	~4.63	~4.66	4.60	4.59
mean deviation from planarity (Å)	0.02	0.03	0.05	0.06	0.05	0.07	0.11	0.03
			0.06		0.06			
Fe shift from porphyrin plane (Å)	0.29	0.49	0.26	0.48	0.26	0.47	0.55	0.49
			0.24	0.46	0.27			
Fe−Fe distance (Å)	9.12	9.04	8.95	8.87	9.03	8.90	9.05	8.94
Fe−O bond length (Å)	1.96	1.90	1.97	1.91	1.96	1.91	1.89	1.84
O−C−O−Fe torsion angle	172.2	171.5	170.1	166.7	169.5	167.5	155.2	167.5
					175.2	171.7		
C−C−C−C torsion angle on propionate bridge	172.1	174.6	175.1	177.0	172.0	176.6	171.2	174.6
			170.3	172.7	170.1	175.5		
C−C−C−C torsion angle on propionic acid	166.0	166.7	170.7	172.0	166.2	166.9	157.3	166.7
			164.4	165.6	168.9	169.3		
H-bond O···O distance (Å)	2.65	2.66	2.68	2.68	2.66	2.67	2.8	2.70
			2.63	2.66	2.65			
				in the unit cell of the minor phase				
interplanar distance (Å)	4.49	4.54	4.35	4.42	~4.55	~4.58		4.57
mean deviation from planarity (Å)	0.02	0.02	0.03	0.02	0.02	0.02		0.03
					0.04	0.03		
Fe shift from porphyrin plane (Å)	0.27	0.46	0.27	0.45	0.26	0.44		0.46
Fe−Fe distance (Å)	9.35	9.34	9.37	9.33	9.26	9.24		9.24
Fe−O bond length (Å)	1.96	1.90	1.96	1.90	1.95	1.90		1.85
					1.96	1.91		
O−C−O−Fe torsion angle	171.6	170.7	174.8	176.2	173.5	175.8		155.7
					176.0	177.9		
C−C−C−C torsion angle on propionate bridge	166.6	165.5	160.3	161.3	168.4	168.1		172.8
					170.5	169.2		
C−C−C−C torsion angle on propionic acid	167.0	168.8	168.4	169.3	168.8	169.7		162.8
					165.7	167.2		
H-bond O···O distance (Å)	2.64	2.65	2.62	2.63	2.65	2.66		2.65
					2.67	2.67		

[a] The interplanar distance, the mean deviation from planarity, and the Fe shift are given with respect to the planes of the porphyrin skeletons without the Fe atom and the side groups, obtained by principal component analysis. Two values are shown if the relaxed structure is not completely symmetric, as a center of symmetry was not imposed. If the planes of the two monomers are not perfectly parallel, the interplanar distance is approximate.

structures of the dimers in the crystal is that in the crystal the bridging propionates are fully extended. This is apparent in the larger Fe−Fe distance in the crystal as well as the C−C−C−C torsion angles on the propionate bridges and the *O* = C−O−Fe-(3+) torsion angles, which are now closer to 180°. This brings the dimer structure obtained from a fully periodic treatment of the β-hematin crystal into a better agreement with the refined structures obtained from X-ray diffraction experiments. This difference may be attributed to the interactions with adjacent dimers that are present in the crystal but not in the isolated dimer, namely, the dispersion interactions and hydrogen bonds. These interactions draw the monomers toward adjacent dimers and away from each other. Another noticeable difference between the relaxed structures of the isolated dimers and those of the dimers in the crystal is that in the isolated dimer, the Fe(3+) PPIX monomers are more buckled. This is reflected in the deviation from planarity. In this respect, the geometry of the dimers in the crystal is in better agreement with the refinement of Straasø et al.,[18] where the structure of the monomer is based on that of a recently reported complex of Fe(3+) PPIX with halofantrine,[75] as compared to the refinement of Pagola et al.,[6] where the structure of the monomer is based on that of α-chlorohemin.[20]

The optimized OH···O distances (in the H-bonds between adjacent dimers) range from 2.62 to 2.68 Å with some variation between the different stereoisomers and the different spin states. The H-bonds in the minor phase unit cell are somewhat shorter than in the major phase unit cell. These results are in excellent agreement with the predominant hydrogen bond length of 2.65 Å, obtained from an analysis of about 5000 species extracted from the Cambridge Database

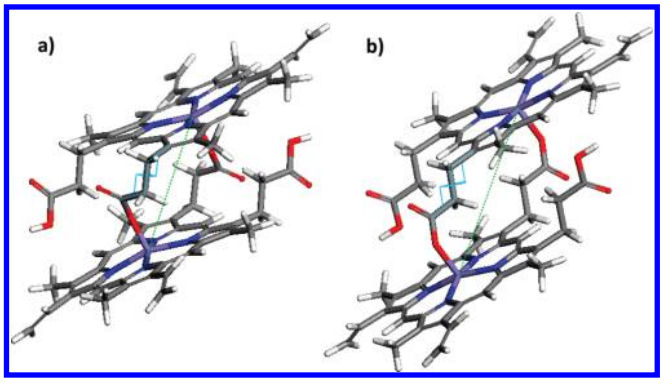

Figure 5. Structure of the $cd\bar{1}_1$ stereoisomer, obtained with PBE+vdW, with $J = 7$ (a) as an isolated dimer and (b) in the major phase unit cell. The Fe−Fe distance and the C−C−C−C torsion angle on the propionate bridge are marked in green and light blue. The differences in the interplanar distance and the planarity of the monomers are clearly visible.

and with the bond length of 2.695 Å obtained by Straasø et al.[18]

On the basis of the results of our calculations regarding the energetics of the different stereoisomers of the Fe(3+) PPIX dimer, we suggest that β-hematin nucleation begins with dimerization via the formation of iron−carboxylate bonds between two Fe(3+) PPIX monomers. At this stage, the most stable $cd\bar{1}_1$ stereoisomer forms predominantly, but because the three isomers are close in energy, the $cd\bar{1}_2$ and $cd2$ stereoisomers may also form in smaller quantities. The stereoisomeric dimers may then interconnect by forming cyclic hydrogen bonds between the free propionate groups and the hydrogen-bonded chains may then form three-dimensional clusters via $\pi-\pi$ interactions. Thus, an ensemble of nuclei of subcritical size that differ in the relative composition of the stereoisomers may form. Because of their higher abundance, precritical nuclei rich in the $cd\bar{1}_1$ dimer would then be more likely to grow into crystals and form the major phase. At this stage, it is likely that because the $cd\bar{1}_2$ stereoisomer is stereochemically mismatched to the faces of the major phase crystal and is less stable in the major phase unit cell, the $cd\bar{1}_2$ dimers would not be occluded into the growing major phase crystal but segregate, leading to the formation of nuclei rich in $cd\bar{1}_2$ dimers, which would grow into the minor phase. From stereochemical considerations, the $cd2$ stereoisomer may match the growing faces of either phase (see further discussion in ref 18). However, energetically the $cd2$ isomer is more stable in the major phase unit cell. Therefore, we suggest that the $cd2$ isomer may be incorporated into the major phase and perhaps to a lesser extent into the minor phase. Thus, a mechanism that begins with the formation of cyclic dimers explains the subsequent formation of two distinct crystalline phases with somewhat different unit cells, associated with different stereoisomers of the Fe(3+) PPIX dimer.

CONCLUSION

We conducted a vdW-corrected DFT study of β-hematin. The geometry and relative stability of the three possible stereoisomers of the Fe(3+) PPIX cyclic dimer were examined for isolated dimers and for crystals with the unit cells of the major and minor phases of β-hematin, as obtained by Straasø et al.[18] The PBEh functional correctly predicts the experimentally observed high spin state, while the PBE functional erroneously predicts a lower spin state. However, the spin state has a minor effect on the geometry and relative stability of the three stereoisomers; therefore, we can draw valid conclusions from the computationally simpler PBE+vdW calculations.

The significance of the vdW correction for treating β-hematin and similar molecular crystals is demonstrated through the markedly different behavior of PBE vs PBE+vdW along the three crystal axes. Along the c-axis, where the binding is mostly due to hydrogen bonds, both PBE and PBE+vdW give a deep minimum and a lattice constant in agreement with experiment. However, along the a- and b-axes, where the binding is predominantly dispersive, PBE gives little or no binding, while PBE+vdW gives lattice constants in good agreement with experiment.

The important role of dispersion is further highlighted by the differences between the geometry of the isolated dimers and that of the dimers in the crystal. For isolated dimers, dispersion interactions bring the two monomers into a greater overlap than that observed for β-hematin crystal in XRD experiments, so that the bridging propionate chains are not fully extended. A fully periodic treatment brings the dimer structure into a better agreement with the refined structures obtained from XRD experiments. This may be attributed to the interactions with adjacent dimers that are present in the crystal but not in the isolated dimer. Dispersion interactions, including $\pi-\pi$ interactions between the porphyrin rings, vdW interactions between the methyl and vinyl side groups, and hydrogen bonds between the free propionic acids, draw the monomers toward adjacent dimers and away from each other.

On the basis of our findings regarding the relative stability of the three stereoisomers as isolated dimers and in the unit cells of the two phases of β-hematin, we suggest a mechanism whereby the first stage of nucleation is the formation of cyclic dimers. In this stage, the formation of the most stable $cd\bar{1}_1$ stereoisomer may be accompanied by the formation of smaller quantities of the less stable $cd\bar{1}_2$ and $cd2$ stereoisomers. In the ensuing crystallization stage, the $cd\bar{1}_1$ stereoisomer forms the major phase. The $cd\bar{1}_2$ dimers are unlikely to adsorb on the growing faces of the major phase crystal due to a stereochemical mismatch. It is therefore reasonable that the $cd\bar{1}_2$ dimers segregate and form the minor phase. From stereochemical considerations, the $cd2$ dimer may be adsorbed to particular faces of either phase. However, we find that the major phase unit cell is energetically favorable for this stereoisomer. Therefore, it may be incorporated into the major phase. Thus, the mechanism that we suggest explains the experimentally observed formation of two distinct crystal phases of β-hematin, with somewhat different unit cells, associated with different stereoisomers of the Fe(3+) PPIX cyclic dimer.

AUTHOR INFORMATION

Corresponding Author

*E-mail: noa@ices.utexas.edu (N.M.); leeor.kronik@weizmann.ac.il (L.K.); leslie.leiserowitz@weizmann.ac.il (L.L.).

ACKNOWLEDGMENT

Parts of this work were financially supported by the Kimmelmann Center and by the Lise Meitner Center for Computational Chemistry. Aurora Cruz Cabeza is thanked for her interest and efforts in the initial stages of the work.

REFERENCES

(1) Sullivan, D. J.; Krishna, S. *Drugs, Disease and Post-Genomic Biology, Current Topics in Microbiology and Immunology*; Springer-Verlag: Berlin, Heidelberg, 2005; Vol. 295.

(2) Sullivan, D. J. J.; Matile, H.; Ridley, R. G.; Goldberg, D. E. *J. Biol. Chem.* **1998**, *273*, 31103–31107.

(3) Buller, R.; Peterson, M. L.; Almarsson, Ö.; Leiserowitz, L. *Cryst. Growth Des.* **2002**, *2*, 553.

(4) Weissbuch, I.; Leiserowitz, L. *Chem. Rev.* **2008**, *108*, 4899.

(5) Sullivan, D. J. J.; Y., G. I.; Russell, D. G.; Goldberg, D. E. *Proc. Natl. Acad. Sci. U.S.A.* **1996**, *93*, 11865–11870.

(6) Pagola, S.; Stephens, P. W.; Bohle, D. S.; Kosar, A. D.; Madsen, S. K. *Nature* **2000**, *404*, 307.

(7) Egan, T. J.; Mavuso, W. W.; Ncokazi, K. K. *Biochemistry* **2001**, *40*, 204–213.

(8) Goldberg, D. E.; Slater, A. F. G.; Cerami, A.; Henderson, G. B. *Proc. Natl. Acad. Sci. U.S.A.* **1990**, *87*, 2931.

(9) Fitch, C. D.; Cai, G. Z.; Shen, Y. F.; Shoemaker, J. D. *Biochim. Biophys. Acta, Mol. Basis Dis.* **1999**, *1454*, 31.

(10) Jackson, K. E.; Klonis, N.; Ferguson, D. J. P.; Adisa, A.; Dogovski, C.; Tilley, L. *Mol. Microbiol.* **2004**, *54*, 109.

(11) Pisciotta, J. M.; Coppens, I.; Tripathi, A. K.; Scholl, P. F.; Schuman, J.; Bajad, S.; Shulaev, V.; Sullivan, D. J. *Biochem. J.* **2007**, *402*, 197.

(12) Egan, T. J.; Chen, J. Y. J.; de Villiers, K. A.; Mabotha, T. E.; Naidoo, K. J.; Ncokazi, K. K.; Langford, S. J.; McNaughton, D.; Pandiancherri, S.; Wood, B. R. *FEBS Lett.* **2006**, *580*, 5105.

(13) de Villiers, K. A.; Osipova, M.; Mabotha, T. E.; Solomonov, I.; Feldman, Y.; Kjaer, K.; Weissbuch, I.; Egan, T. J.; Leiserowitz, L. *Cryst. Growth Des.* **2009**, *9*, 626.

(14) Bohle, D. S.; Kosar, A. D.; Stephens, P. W. *Acta Crystallogr.* **2002**, *D58*, 1752–1756.

(15) (a) Egan, T. J. *J. Inorg. Biochem.* **2008**, *102*, 1288–1299. (b) *Mol. Biochem. Parasitol.* **2008**, *157*, 127–136.

(16) Scheidt, W. R.; Lee, Y. J. *Structure & Bonding*; Springer: Berlin/Heidelberg: 1987; Vol. 64, p 1.

(17) The *cd*2 isomer has two enantiomers, denoted by Straasø et al.[18] as *cd*2(−) and *cd*2(+). Here, we treat only the *cd*2(−) enantiomer, based on the assumption that the two enantiomers are identical for all practical purposes.

(18) Straasø, T.; Kapishnikov, S.; Kato, K.; Takata, M.; Als-Nielsen, J.; Leiserowitz, L. *Cryst. Growth Des.* **2011**, *11*, DOI: 10.1021/cg200410b.

(19) Klonis, N.; Dilanian, R.; Hanssen, E.; Darmanin, C.; Streltsov, V.; Deed, S.; Quiney, H.; Tilley, L. *Biochemistry* **2010**, *49*, 6804–6811.

(20) Koenig, D. F. *Acta Crystallogr.* **1965**, *18*, 663.

(21) Koch, W.; Holthausen, M. C. *A Chemist's Guide to Density Functional Theory*; Wiley-VCH: Weinheim, Germany: 2001; Chapter 12.

(22) del Río, D.; Sarangi, R.; Chufán, E. E.; Karlin, K. D.; Hedman, B.; Hodgson, K. O.; Solomon, E. I. *J. Am. Chem. Soc.* **2005**, *127*, 11969.

(23) Silaghi-Dumitrescu, R. *J. Mol. Struct. Theochem* **2005**, *722*, 233–237.

(24) Smith, D. M. A.; Dupuis, M.; Straatsma, T. P. *Mol. Phys.* **2005**, *103*, 273–278.

(25) Scherlis, D. A.; Cococcioni, M.; Sit, P.; Marzari, N. *J. Phys. Chem. B* **2007**, *111*, 7384–7391.

(26) Strickland, N.; Harvey, J. N. *J. Phys. Chem. B* **2007**, *111*, 841–852.

(27) Yoshioka, Y.; Satoh, H.; Mitani, M. *J. Inorg. Biochem.* **2007**, *101*, 1410–1427.

(28) Khvostichenko, D.; Choi, A.; Boulatov, R. *J. Phys. Chem. A* **2008**, *112*, 3700–3711.

(29) Praneeth, V. K. K.; Paulat, F.; Berto, T. C.; DeBeer George, S.; Näther, C.; Sulok, C. D.; Lehnert, N. *J. Am. Chem. Soc.* **2008**, *130*, 15288–15303.

(30) Radon, M.; Pierloot, K. *J. Phys. Chem. A* **2008**, *112*, 11824–11832.

(31) Shoji, M.; Isobe, H.; Saito, T.; Kitagawa, Y.; Yamanaka, S.; Kawakami, T.; Okumura, M.; Yamaguchi, K. *Int. J. Quantum Chem.* **2008**, *108*, 2950–2965.

(32) Abdurahman, A.; Renger, T. *J. Phys. Chem. A* **2009**, *113*, 9202–9206.

(33) Oláh, J.; Harvey, J. N. *J. Phys. Chem. A* **2009**, *113*, 7338–7345.

(34) Porro, C. S.; Kumar, D.; de Visser, S. P. *Phys. Chem. Chem. Phys.* **2009**, *11*, 10219–10226.

(35) Rydberg, P.; Olsen, L. *J. Phys. Chem. A* **2009**, *113*, 11949.

(36) Vancoillie, S.; Zhao, H.; Radon, M.; Pierloot, K. *J. Chem. Theory Comput.* **2010**, *6*, 576–582.

(37) Galstyan, A. S.; Zarić, S. D.; Knapp, E. W. *J. Biol. Inorg. Chem.* **2005**, *10*, 343–354.

(38) De Angelis, F.; Car, R.; Spiro, T. G. *J. Am. Chem. Soc.* **2003**, *125*, 15710–15711.

(39) Jensen, K. P.; Ryde, U. *J. Biol. Chem.* **2004**, *279*, 14561–14569.

(40) Jensen, K. P.; Roos, B. O.; Ryde, U. *J. Inorg. Biochem.* **2005**, *99*, 45–54.

(41) Radon, M.; Broclawik, E.; Pierloot, K. *J. Phys. Chem. B* **2010**, *114*, 1518–1528.

(42) Liao, M. S.; Huang, M. J.; Watts, J. D. *J. Phys. Chem. A* **2010**, *114*, 9554–9569.

(43) Saito, T.; Kataoka, Y.; Nakanishi, Y.; Matsui, T.; Kitagawa, Y.; Kawakami, T.; Okumura, M.; Yamaguchi, K. *J. Mol. Struct. Theochem* **2010**, *954*, 98–104.

(44) Zhang, F.; Ai, Y. J.; Luo, Y.; Fang, W. H. *J. Phys. Chem. A* **2010**, *114*, 1980–1984.

(45) Siegbahn, P. E. M.; Blomberg, M. R. A.; Chen, S. L. *J. Chem. Theory Comput.* **2010**, *6*, 2040–2044.

(46) Araújo, J. Q.; Carneiro, J. W. D.; Araujo, M. T.; Leited, F. H. A.; Tarantod, A. G. *Bioorg. Med. Chem.* **2008**, *16*, 5021–5029.

(47) Feng, X. T.; Yu, J. G.; Lei, M.; Fang, W. H.; Liu, S. *J. Phys. Chem. B* **2009**, *113*, 13381.

(48) Kamiya, K.; Yamamoto, S.; Shiraishi, K.; Oshiyama, A. *J. Phys. Chem. B* **2009**, *113*, 6866–6872.

(49) Sena, A. M. P.; Brázdová, V.; Bowler, D. R. *Phys. Rev. B* **2009**, *79*, 245404.

(50) Charkin, O. P.; Klimenko, N. M.; Charkin, D. O.; Chang, H.-C.; Lin, S.-H. *J. Phys. Chem. A* **2007**, *111*, 9207.

(51) Tkatchenko, A.; Romaner, L.; Hofmann, O. T.; Zojer, E.; Ambrosch-Draxl, C.; Scheffler, M. *MRS Bull.* **2010**, *35*, 435.

(52) Riley, K. E.; Pitonak, M.; Jurecka, P.; Hobza, P. *Chem. Rev.* **2010**, *110*, 5023.

(53) Tkatchenko, A.; Scheffler, M. *Phys. Rev. Lett.* **2009**, *102*, 073005.

(54) Marom, N.; Tkatchenko, A.; Scheffler, M.; Kronik, L. *J.Chem. Theory Comput.* **2010**, *6*, 81.

(55) Santra, B.; Michaelides, A.; Fuchs, M.; Tkatchenko, A.; Filippi, C.; Scheffler, M. *J. Chem. Phys.* **2008**, *129*, 194111.

(56) Tkatchenko, A.; Rossi, M.; Blum, V.; Ireta, J.; Scheffler, M. To be published.

(57) Tkatchenko, A.; Rossi, M.; Blum, V.; Ireta, J.; Scheffler, M. *Phys. Rev. Lett.* **2011**, *106*, 118102.

(58) Mercurio, G.; McNellis, E. R.; Martin, I.; Hagen, S.; Leyssner, F.; Soubatch, S.; Meyer, J.; Wolf, M.; Tegeder, P.; Tautz, F. S.; Reuter, K. *Phys. Rev. Lett.* **2010**, *104*, 036102.

(59) Lee, Y.-L.; Kim, S.; Park, C.; Ihm, J.; Son, Y.-W. *ACS Nano* **2010**, *4*, 1345.

(60) Marom, N.; Bernstein, J.; Garel, J.; Tkatchenko, A.; Joselevich, E.; Kronik, L.; Hod, O. *Phys. Rev. Lett.* **2010**, *105*, 046801.

(61) (a) Perdew, J. P.; Burke, K.; Ernzerhof, M. *Phys. Rev. Lett.* **1996**, *77*, 3865. (b) Perdew, J. P.; Burke, K.; Ernzerhof, M. *Phys. Rev. Lett.* **1997**, *78*, 1396 (E).

(62) Perdew, J. P.; Ernzerhof, M.; Burke, K. *J. Chem. Phys.* **1996**, *105*, 9982.

(63) (a) Adamo, C.; Barone, V. *J. Chem. Phys.* **1999**, *110*, 6158. (b) Ernzerhof, M.; Scuseria, G. E. *J. Chem. Phys.* **1999**, *110*, 5029.

(64) (a) Blum, V.; Gehrke, R.; Hanke, F.; Havu, P.; Havu, V.; Ren, X.; Reuter, K.; Scheffler, M. *Comput. Phys. Commun.* **2009**, *180*, 2175.(b) FHI-aims—Theory Department—Fritz-Haber Institute Berlin; http://www.fhi-berlin.mpg.de/aims/.

(65) Havu, V.; Blum, V.; Havu, V.; Scheffler, M. *J. Comput. Phys.* **2009**, *228*, 8367–8379.
(66) To decrease the memory requirements of the PBEh calculations, the tier2 basis set was truncated by eliminating f, g, and h basis functions, with a negligible effect on the accuracy.
(67) Behler, J.; Delley, B.; Lorenz, S.; Reuter, K.; Scheffler, M. *Phys. Rev. Lett.* **2005**, *94*, 036104.
(68) Behler, J.; Delley, B.; Reuter, K.; Scheffler, M. *Phys. Rev. B* **2007**, *75*, 115409.
(69) Sienkiewicz, A.; Krzystek, J.; Vileno, B.; Chatain, G.; Kosar, A. J.; Bohle, D. S.; Forró, L. *J. Am. Chem. Soc.* **2006**, *128*, 4534–4535.
(70) Bohle, D. S.; Debrunner, P.; Jordan, P. A.; Madsen, S. K.; Schulz, C. E. *J. Am. Chem. Soc.* **1998**, *120*, 8255–8256.
(71) Rong, C.; Lian, S.; Yin, D.; Shen, B.; Zhong, A.; Bartolotti, L.; Liu, S. *J. Chem. Phys.* **2006**, *125*, 174102.
(72) Marom, N.; Kronik, L. *Appl. Phys. A: Mater. Sci. Process.* **2009**, *95*, 165.
(73) Because of a later rerefinement of the XRD data, the cell parameters reported by Straasø et al.[18] are slightly different than those used herein.
(74) In ref 14, Bohle et al. report three X-ray powder patterns prepared by different protocols: One is purely the major phase of β-hematin; the second contains two phases, which are the major and minor phases observed by Straasø et al.;[18] and the third, which is a powder pattern, exhibiting poor crystallinity, very different from that of the major or minor phase, may contain a third phase. However, this has not been verified.
(75) de Villiers, K. A.; Marques, H. M.; Egan, T. J. *J. Inorg. Biochem.* **2008**, *102*, 1660.